ARTHRITIS & RHEUMATISM
Vol. 60, No. 10, October 2009, pp 3061–3071
DOI 10.1002/art.24817

Induction of an Antiinflammatory Effect and Prevention of Cartilage Damage in Rat Knee Osteoarthritis by CF101 Treatment

S. Bar-Yehuda,[1] L. Rath-Wolfson,[2] L. Del Valle,[3] A. Ochaion,[1] S. Cohen,[1] R. Patoka,[1] G. Zozulya,[1] F. Barer,[1] E. Atar,[2] S. Piña-Oviedo,[3] G. Perez-Liz,[3] D. Castel,[1] and P. Fishman[1]

Objective. **Studies have suggested that rheumatoid arthritis (RA) and osteoarthritis (OA) share common characteristics. The highly selective A_3 adenosine receptor agonist CF101 was recently defined as a potent antiinflammatory agent for the treatment of RA. The purpose of this study was to examine the effects of CF101 on the clinical and pathologic manifestations of OA in an experimental animal model.**

Methods. **OA was induced in rats by monosodium iodoacetate, and upon disease onset, oral treatment with CF101 (100 μg/kg given twice daily) was initiated. The A_3 adenosine receptor antagonist MRS1220 (100 μg/kg given twice daily) was administered orally, 30 minutes before CF101 treatment. The OA clinical score was monitored by knee diameter measurements and by radiographic analyses. Histologic analyses were performed following staining with hematoxylin and eosin, Safranin O–fast green, or toluidine blue, and histologic changes were scored according to a modified Mankin system. Signaling proteins were assayed by Western blotting; apoptosis was detected via immunohistochemistry and TUNEL analyses.**

Results. **CF101 induced a marked decrease in knee diameter and improved the changes noted on radiographs. Administration of MRS1220 counteracted the effects of CF101. CF101 prevented cartilage damage, osteoclast/osteophyte formation, and bone destruction. In addition, CF101 markedly reduced pannus formation and lymphocyte infiltration. Mechanistically, CF101 induced deregulation of the NF-κB signaling pathway, resulting in down-regulation of tumor necrosis factor α. Consequently, CF101 induced apoptosis of inflammatory cells that had infiltrated the knee joints; however, it prevented apoptosis of chondrocytes.**

Conclusion. **CF101 deregulated the NF-κB signaling pathway involved in the pathogenesis of OA. CF101 induced apoptosis of inflammatory cells and acted as a cartilage protective agent, which suggests that it would be a suitable candidate drug for the treatment of OA.**

Osteoarthritis (OA) is the most common chronic joint disease. Articular cartilage is a major component of the joint, and its mechanical properties depend on the integrity of the extracellular matrix, which is composed mainly of proteoglycans and collagens. Degeneration of joint cartilage is the central feature in OA, but the disease is associated with concomitant changes in synovium and subchondral bone metabolism, causing inflammation of the synovial membrane in the involved joints (1).

The cause of OA is multifactorial and includes both systemic and local biomechanical factors (2). Systemic factors that have been associated with OA include age, sex, race- and gene-based susceptibility, bone density, estrogen levels, and nutritional factors. OA results from the failure of chondrocytes that lie within the joint to synthesize a good-quality matrix and to maintain a balance between synthesis and degradation of the extracellular matrix. Synovial inflammation and local concentration of proinflammatory mediators seem to

Supported by Can-Fite BioPharma.

[1]S. Bar-Yehuda, PhD, A. Ochaion, MSc, S. Cohen, MSc, R. Patoka, MSc, G. Zozulya, MSc, F. Barer, PhD, D. Castel, DVM, P. Fishman, MD: Can-Fite BioPharma, Petah Tikva, Israel; [2]L. Rath-Wolfson, MD, E. Atar, MD: Rabin Medical Center and Tel Aviv University, Petah Tikva, Israel; [3]L. Del Valle, MD, S. Piña-Oviedo, MD, G. Perez-Liz, MD: Temple University School of Medicine, Philadelphia, Pennsylvania.

Drs. Bar-Yehuda, Rath-Wolfson, and Del Valle contributed equally to this work.

Address correspondence and reprint requests to P. Fishman, MD, Can-Fite BioPharma, 10 Bareket Street, PO Box 7537, Petah Tikva 49170, Israel. E-mail: pninia@canfite.co.il.

Submitted for publication December 21, 2008; accepted in revised form June 15, 2009.

be directly involved in the generation of pain in OA joints (3–5).

The medications most commonly used to treat OA are symptom-modifying drugs, such as nonsteroidal antiinflammatory drugs (NSAIDs) and cyclooxygenase 2 inhibitors. These treatments have been shown to be effective for improving levels of pain and disability, but they are not disease-modifying drugs (6).

While OA has traditionally been defined as a nonautoimmune joint disease, many studies have highlighted the critical role of synovial inflammation in the progression of this disease (7–9). The progressive destruction of the articular cartilage, which results from an imbalance between the anabolic and catabolic processes, is a common feature of rheumatoid arthritis (RA) and OA. Recent studies have also shown that similar to their roles in RA, NF-κB and tumor necrosis factor α (TNFα) play a predominant role in the etiology and pathogenesis of OA (10). In addition, the pathophysiologic responses of the synovial tissue and the joint cartilage in OA resemble those manifested in RA (8,11).

The G_i protein–associated A_3 adenosine receptor was recently defined as a novel antiinflammatory target. This receptor is overexpressed in synovial cells and peripheral blood mononuclear cells (PBMCs) from patients with RA, and agonists to this receptor act as potent antiinflammatory agents.

Our previous studies showed that the A_3 adenosine receptor is highly expressed in inflammatory cells derived from the synovium of rats with adjuvant-induced arthritis (AIA), as well as from the synovium of RA patients. Interestingly, receptor overexpression is also reflected in the PBMCs, reflecting receptor status in the remote sites of inflammation (12–16).

Based on these findings, synthetic highly selective agonists to the A_3 adenosine receptor were introduced for the treatment of AIA. CF101, which is known chemically as 1-deoxy-1-[6-[[(3-iodophenyl)methyl] amino]-9*H*-9-yl]-*N*-methyl-β-D-ribofuranuronamide (IB-MECA), and CF502, which is known chemically as [(1′*R*,2′*R*,3′*S*,4′*R*,5′*S*)-4-{2-chloro-6-[(3-chlorophenyl methyl)amino]purin-9-yl}-1-(methylaminocarbonyl) bicyclo-[3.1.0]hexane-2,3-diol] (MRS3558), induced marked amelioration of the clinical and pathologic manifestations of AIA (12–18). Mechanistically, the agonists were shown to decrease the expression levels of phosphatidylinositol 3-kinase (PI3K), protein kinase B (PKB)/Akt, IKKα/β, and IκB, which resulted in down-regulation of NF-κB, inhibition of TNFα, and apoptosis of inflammatory cells (12). In addition, CF101 down-regulated the expression levels of RANKL, preventing bone and cartilage destruction (13).

These data prompted the initiation of preclinical and clinical programs using CF101 as a candidate anti-inflammatory drug. In a phase I study in healthy subjects, CF101 was found to be safe and well tolerated and to have a linear pharmacokinetic activity (19). In a phase IIa study of patients with RA, CF101 administered orally twice a day for 12 weeks resulted in an improvement of the signs and symptoms of RA and appeared to act as a disease-modifying antirheumatic drug. In these studies, CF101 was found to be safe and very well tolerated (20).

The marked antiinflammatory effect of CF101 in RA, together with its impressive safety profile and oral bioavailability, led us to explore its effect in an in vivo model of OA.

MATERIALS AND METHODS

Reagents. Monosodium iodoacetate (MIA; Sigma, St. Louis, MO) was prepared in saline solution. The A_3 adenosine receptor agonist IB-MECA, which was designated CF101, was synthesized for Can-Fite BioPharma by Albany Molecular Research (Albany, NY). A stock solution was prepared in DMSO and was further diluted in phosphate buffered saline (PBS). The A_3 adenosine receptor antagonist MRS1220 was purchased from Sigma-RBI (Natick, MA). A stock solution was prepared in DMSO and further diluted in PBS.

Rabbit polyclonal antibodies against rat A_3 adenosine receptor (developed against amino acids 151–230 with the internal region of the A_3 adenosine receptor; Santa Cruz Biotechnology, Santa Cruz, CA) and the following signaling proteins were used: PKB/Akt (PKB/Akt phosphorylated at pSer; Sigma, St. Louis, MO), IKKα/β (rabbit polyclonal antibody against amino acids 470–755 of IKKα/β; Santa Cruz Biotechnology), IκBα (rabbit polyclonal antibody against a peptide at the C-terminus of IκBα; Santa Cruz Biotechnology), NF-κB (NF-κB p65-RelA; Chemicon, Temecula, CA), TNFα (rat anti-TNFα; R&D Systems, Minneapolis, MN), Bax (B-9 monoclonal antibody against amino acids 1–171 of Baxα; Santa Cruz Biotechnology), caspase 3 (cleaved caspase 3 [Asp^{175}] antibody, which detects endogenous large fragments [17/19 kd] of activated caspase 3 resulting from cleavage adjacent to Asp^{175}; Cell Signaling Technology, Beverly, MA), β-actin (Santa Cruz Biotechnology), and GAPDH (Santa Cruz Biotechnology).

Experimental model of MIA-induced OA in rats. Male Wistar rats weighing 150–175 gm were obtained from Harlan Laboratories (Jerusalem, Israel). Rats were maintained on a standardized pelleted diet and were supplied with tap water. Experiments were performed in accordance with the guidelines established by the Institutional Animal Care and Use Committee at Can-Fite BioPharma (Petah Tikva, Israel).

OA was induced with 2 mg of MIA in a total volume of 50 μl. MIA was injected intraarticularly through the patellar ligament of the right knee, using a 26-gauge needle, while the

rat was under anesthesia. The left knee joint (control) was injected with saline.

Oral treatment with CF101 (100 μg/kg given twice a day) was started on day 7 after MIA injection and was continued until the study was terminated on day 22. Another group of rats was administered MRS1220 (100 μg/kg given twice a day) orally 30 minutes before each CF101 treatment. The control group was treated with vehicle alone. Each experimental group included 10 animals, and the experiments were performed 3 times. The diameter of the knees was measured every other day using digital calipers (Mitotoyo, Tokyo, Japan).

Radiographic examination. At the end of the study, animals in each treatment group were euthanized, their legs were dissected, and the surrounding soft tissue was removed. Radiographs of all limbs were obtained with an ordinary x-ray machine (Optimus; Philips, Best, The Netherlands) and film cassettes. All limbs were x-rayed in 2 projections and in the same manner by the same radiographer. The radiographic images were examined by 2 experienced radiologists.

Histopathologic analysis. The knee joints of the rats were dissected, and the surrounding soft tissue was removed. The tissues were fixed in 10% buffered formalin, decalcified in hydrochloric acid (CalciClear Rapid; National Diagnostics, Atlanta, GA), and embedded in paraffin. Sections (5μ in thickness) were cut and stained with hematoxylin and eosin (H&E) for routine histologic evaluation. Additional sections were rehydrated in a graded series of ethanol and stained with Safranin O–fast green to identify proteoglycans or with toluidine blue to evaluate cartilage damage and osteophytes.

Cartilage damage was evaluated according to the depth and extent of the damage. The depth was scored on a scale of 0–5, where 0 = normal, 1 = minimal, affecting the superficial zone only, 2 = mild invasion into the upper middle zone only, 3 = moderate invasion well into the middle zone, 4 = marked invasion into the deep zone but not to the tidemark, and 5 = severe full-thickness degradation to the tidemark. The extent of tibial plateau involvement was scored as 1 (minimal), 2 (moderate), or 3 (severe).

A modified Mankin system (21) was also used to score cartilage changes, as follows: structure was scored on a scale of 0–6, where 0 = normal, 1 = irregular surface, including fissures into the radial layer, 2 = pannus, 3 = absence of superficial cartilage layers ($\geq$6), 4 = slight disorganization (cellular row absent, some small superficial clusters), 5 = fissure into the calcified cartilage layer, and 6 = disorganization (chaotic structure, clusters, and osteoclasts activity); cellular abnormalities were scored on a scale of 0–3, where 0 = normal, 1 = hypercellularity, including small superficial clusters, 2 = clusters, and 3 = hypocellularity; and matrix staining was scored on a scale of 0–4, where 0 = normal/slight reduction of staining, 1 = staining reduced in the radial layer, 2 = staining reduced in the interterritorial matrix, 3 = staining present only in the pericellular matrix, and 4 = staining absent.

In addition, the extent of inflammation was scored on a scale of 0–4, based on the degree of cellular infiltration into the tissue, where 0 = normal (no infiltrates), 1 = minimal inflammatory cell infiltration, 2 = mild infiltration, 3 = moderate infiltration, and 4 = marked infiltration. Pannus formation in the joint tissues and synovial lining cell hyperplasia were scored on a scale of 0–4, where 0 = normal, 1 = minimal loss of cortical bone at a few sites, 2 = mild loss of cortical trabecular bone, 3 = moderate loss of bone at many sites, and 4 = marked loss of bone at many sites, with fragmenting and full-thickness penetration of the inflammatory process or the pannus formation into the cortical bone. Osteoclasts were scored on a scale of 0–4, where 0 = normal (essentially no osteoclasts), 1 = few osteoclasts (lining $<$5% of most affected bone surfaces), 2 = some osteoclasts (lining 2–25% of most affected bone surfaces), 3 = many osteoclasts (lining 26–50% of most affected bone surfaces), and 4 = myriad osteoclasts (lining $>$50% of most affected bone surfaces).

The mean of the scores for all histologic parameters we assessed was calculated. This value was designated as the histology score.

Preparation of protein extracts. On days 15 and 22, rats were treated with CF101 or vehicle and were killed 2 hours later. The knees were dissected above the ankle joint, and the bony tissue was broken into pieces and mixed with radioimmunoprecipitation assay (RIPA) extraction buffer containing 150 m*M* NaCl, 50 m*M* Tris, 1% Nonidet P40, 0.5% deoxycholate, and 0.1% sodium dodecyl sulfate (SDS). Tissues were then homogenized on ice with a Polytron homogenizer. The samples were rinsed with ice-cold PBS and transferred to ice-cold lysis buffer (RIPA buffer, consisting of 50 m*M* Tris buffer, pH 7.5, 150 m*M* NaCl, 1% Nonidet P40, 0.5% deoxycholate, and 0.1% SDS). Cellular debris was removed by centrifugation for 10 minutes at 7,500*g*. Protein concentrations were determined with the use of a protein assay dye reagent from Bio-Rad (Richmond, CA).

Western blot analysis. Western blotting was performed according to the following protocol. Equal amounts of protein (50 μg) were separated by SDS–polyacrylamide gel electrophoresis on 10% polyacrylamide gels (Invitrogen, San Diego, CA). The resolved proteins were then electroblotted onto nitrocellulose membranes (Schleicher & Schuell, Keene, NH). Membranes were blocked with 3% nonfat milk and incubated for 24 hours at 4°C with the desired primary antibody (1:1,000 dilution). Blots were then washed and incubated for 1 hour at room temperature with a secondary antibody (0.1% nonfat milk). Bands were recorded using a BCIP/nitroblue tetrazolium color development kit (Promega, Madison, WI). Data were normalized against the housekeeping protein (β-actin or GAPDH). Results presented below are representative of at least 3 different experiments.

Immunohistochemical analysis. Sections of knee samples obtained from rats with MIA-induced OA were deparaffinized in xylene (3 times for 30 minutes each). The tissues were then hydrated in serial dilutions of ethanol, followed by antigen retrieval upon heating with citrate buffer at 95°C for 30 minutes. Slides were allowed to cool and were then washed 3 times in PBS. Endogenous peroxidase quenching was performed by treating the sections for 20 minutes with fresh 20% hydrogen peroxide in methanol. The sections were then blocked by incubation for 2 hours in 5% normal goat serum (for rabbit polyclonal antibodies) or normal horse serum (for mouse monoclonal antibodies). Then, sections were incubated overnight at room temperature in a humidified chamber with primary antibodies diluted in 0.1% PBS–bovine serum albumin (BSA).

Primary antibodies used in this study included a 1:500

dilution of rabbit polyclonal anti–A_3 adenosine receptor (catalog no. NLS686; Novus Biologicals, Littleton, CO) and a 1:100 dilution of mouse monoclonal anti–caspase 3 (clone E-8; Santa Cruz Biotechnology). After washing 3 times in 1× PBS, the slides were incubated for 1 hour at room temperature with 0.5% biotinylated secondary antibody in 0.1% PBS–BSA and then subjected to 3,3′-diaminobenzidine staining.

TUNEL assay. Apoptosis was examined via DNA fragmentation using a TUNEL assay and ApopTag techniques according to the manufacturer's instructions (ApopTag Peroxidase In Situ Detection kit; Chemicon). Briefly, sections were deparaffinized, rehydrated, and endogenous peroxidase–quenched as described for the immunohistochemical analysis. Slides were pretreated with proteinase K for 15 minutes at room temperature, treated with an equilibration buffer for 10 seconds, and then treated with the enzyme terminal deoxynucleotidyl transferase for 1 hour. The sections were incubated with an antidigoxigenin conjugate, washed with PBS, developed with diaminobenzidine, counterstained with hematoxylin, and then mounted.

Statistical analysis. The results were evaluated using Student's *t*-test. P values less than 0.05 were considered significant. All data are reported as the mean ± SEM. The mean values from different experiments were compared by analysis of variance.

RESULTS

Effect of CF101 on the development of MIA-induced OA. An experimental animal model of MIA-induced OA was used to evaluate the effects of CF101 treatment on the development of the clinical and pathologic manifestations of the disease. In order to evaluate tissue swelling, the diameter of both the MIA-injected and the saline-injected (control) knee joints was measured. The difference between the right (MIA-injected) knee and the left (saline-injected) knee in each animal in the CF101-treated and the vehicle-treated groups was calculated. In the CF101-treated group, the difference between the diameter of the MIA- and saline-injected knees was statistically significantly lower than that in the vehicle-treated group (mean ± SEM percentage inhibition 76.11 ± 4.59; $P < 0.001$). In the group treated with the A_3 adenosine receptor antagonist MRS1220, the results were similar to those in the vehicle-treated group, demonstrating that the antagonist counteracted the effects of CF101 (Figure 1a).

Radiographic examination revealed marked differences between the vehicle-treated and the CF101-treated animals. Sclerotic regions adjacent to the tibioepiphyseal margin, thinning of the epiphysis, and a small exophite were evident in the vehicle-treated animals, whereas in the CF101-treated animals, a normal tibioepiphyseal margin without sclerosis was noted. Images of legs from 3 different animals treated with vehicle and

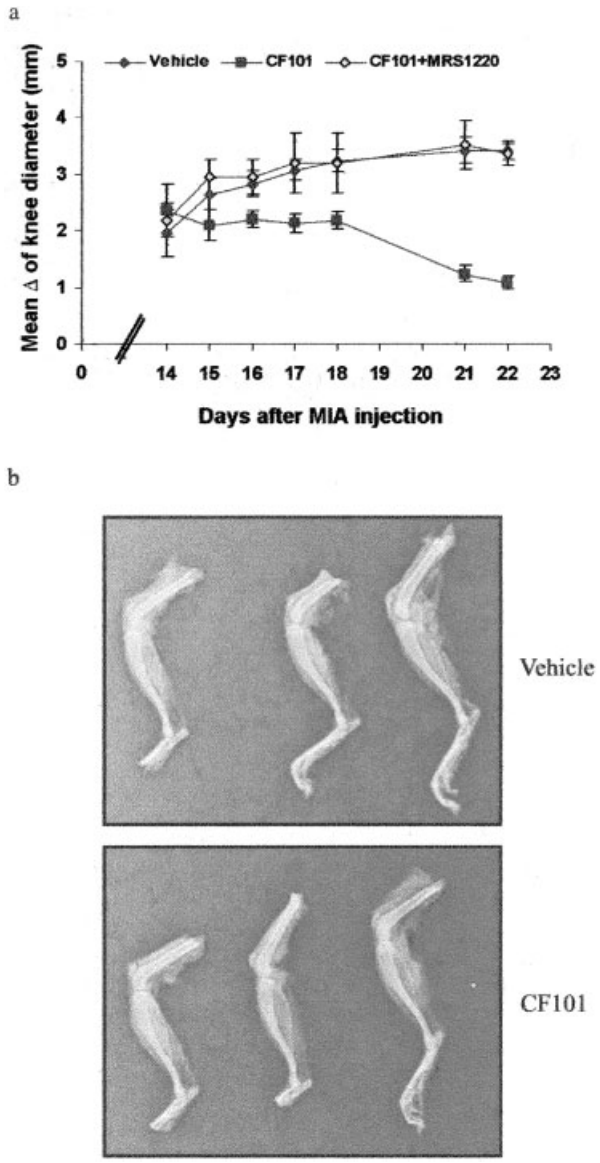

Figure 1. Effect of CF101 on the clinical manifestations of osteoarthritis (OA) in rats. An experimental model of OA in rats was induced by intraarticular injection of monosodium iodoacetate (MIA) into the right knee joint; the left knee joint was injected with saline. Oral treatment with vehicle alone, with CF101 (100 μg/kg given twice a day), or with CF101 plus MRS1220 (100 μg/kg given twice a day; administered 30 minutes before each CF101 treatment) was initiated on day 7. **a,** Mean change in knee joint diameter, as measured every other day using digital calipers. The difference between the MIA-injected knees and the vehicle-injected knees was calculated for each rat. CF101 treatment inhibited the development of knee OA ($P < 0.05$), whereas the addition of MRS1220 counteracted this effect. Values are the mean ± SEM change in knee joint diameter from 3 experiments (n = 10 joints per group). **b,** Radiographs of legs harvested from 3 different vehicle-treated rats and 3 different CF101-treated rats. CF101 treatment preserved the tibial epiphyseal structure and prevented sclerosis. Representative images are shown.

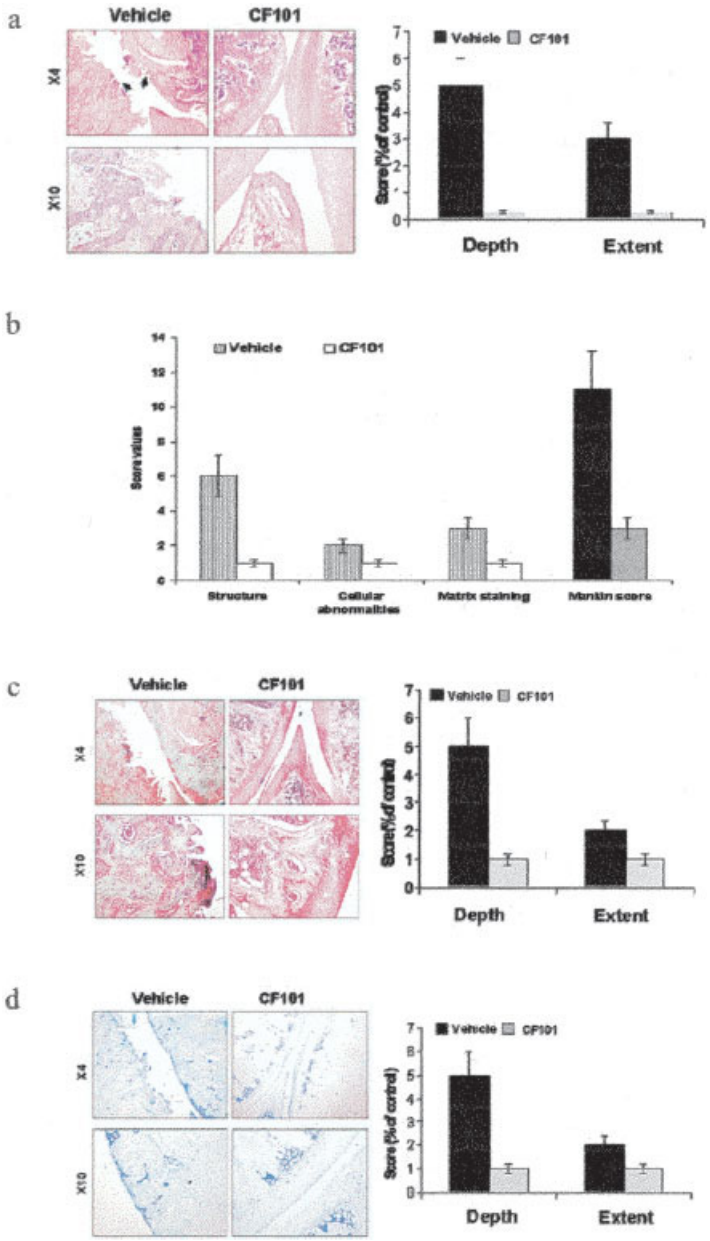

Figure 2. Histopathologic evaluation of knee cartilage from rats with monosodium iodoacetate–induced osteoarthritis (OA) treated with CF101 or vehicle. **a,** Histologic features of cartilage (left) and the depth and extent of cartilage damage (right) in hematoxylin and eosin–stained, paraffin-embedded knee joint sections from OA rats treated with CF101 or vehicle. Extensive cartilage degradation, bone destruction, and fibrosis are seen in vehicle-treated rats, whereas CF101 treatment preserved the articular space and prevented cartilage degeneration. CF101 treatment also markedly decreased the depth and the extent of cartilage damage ($P < 0.05$). **b,** Mankin scores for cartilage structure, cellular abnormalities, and matrix staining, as well as overall Mankin scores, in rats treated with CF101 or vehicle. CF101 prevented damage to the cartilage structure, reduced cellular abnormalities, and preserved matrix staining ($P < 0.05$). **c,** Histologic features of cartilage (left) and the depth and extent of cartilage damage (right) in Safranin O–fast green–stained, paraffin-embedded knee joint sections from OA rats treated with CF101 or vehicle. Extensive cartilage destruction and disappearance of chondrocytes are seen in vehicle-treated rats, whereas CF101 treatment preserved the cartilage structure. CF101 treatment also reduced the depth and extent of cartilage damage ($P < 0.05$). **d,** Histologic features of cartilage (left) and the depth and extent of cartilage damage (right) in toluidine blue–stained, paraffin-embedded knee joint sections from OA rats treated with CF101 or vehicle. Loss of cartilage is seen in vehicle-treated rats, whereas the cartilage is well preserved following CF101 treatment. CF101 treatment also decreased the depth and extent of cartilage damage ($P < 0.05$). Representative images are shown in **a**, **c**, and **d**. Values are the mean ± SEM of pooled data from 3 independent experiments (n = 10 joints per group).

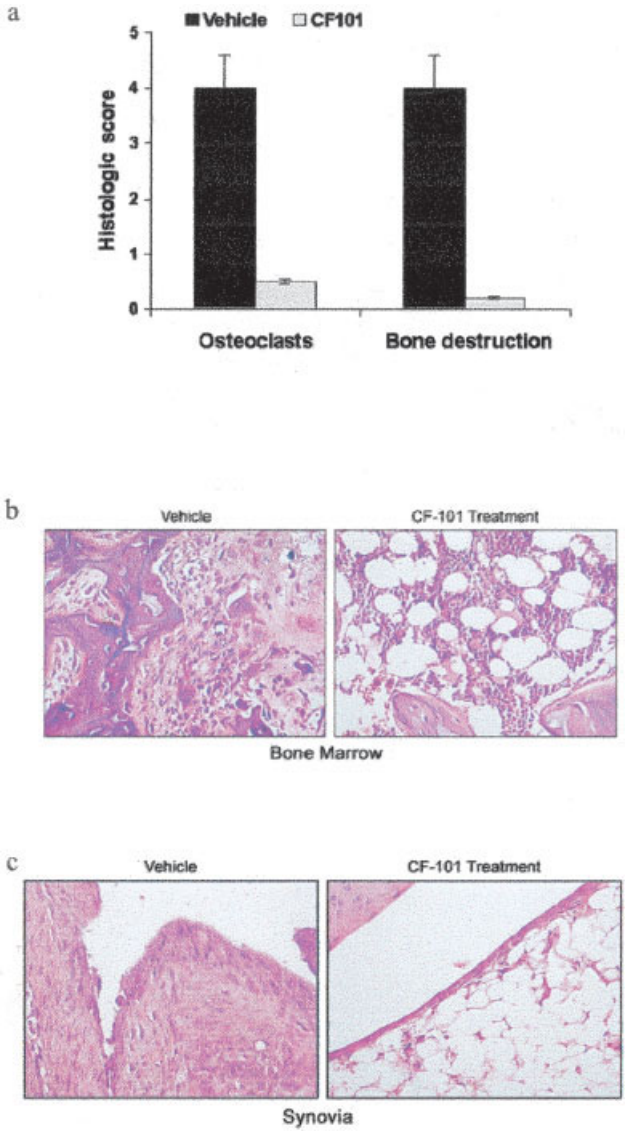

Figure 3. Effect of CF101 treatment on bone and synovium in the knee joints of rats with monosodium iodoacetate–induced osteoarthritis (OA). Bone formation was evaluated in hematoxylin and eosin–stained, paraffin-embedded knee joint sections from OA rats treated with CF101 or vehicle. **a,** Histologic score for osteoclasts and bone destruction in rats treated with CF101 or vehicle. CF101 markedly reduced osteoclast formation and bone destruction ($P < 0.05$). Values are the mean ± SEM of pooled data from 3 independent experiments (n = 10 joints per group). **b,** Histologic features of bone marrow from OA rats treated with CF101 or vehicle. In the vehicle-treated rat, the bone marrow is extensively infiltrated with osteoclasts, whereas in the CF101-treated rat, the bone marrow is preserved. **c,** Histologic features of synovium from OA rats treated with CF101 or vehicle. In the vehicle-treated rat, there is massive proliferation of synovial cells, whereas in the CF101-treated rat, the synovial membrane is preserved. Representative images are shown in **b** and **c** (original magnification × 20).

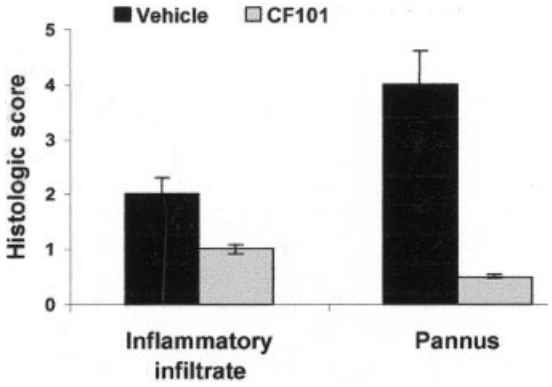

Figure 4. Effect of CF101 on features of inflammation in the knee joints of rats with monosodium iodoacetate–induced osteoarthritis (OA). Histologic scores for inflammatory infiltrate and pannus were determined in hematoxylin and eosin–stained, paraffin-embedded knee joint sections from OA rats treated with CF101 or with vehicle. Lymphocyte infiltration and pannus formation in the articular space were markedly inhibited upon CF101 treatment ($P < 0.05$). Values are the mean ± SEM of pooled data from 3 independent experiments (n = 10 joints per group).

from 3 different animals treated with CF101 are shown in Figure 1b.

Effect of CF101 on the histologic manifestations of OA. H&E analysis of the MIA-injected knees revealed that in the vehicle-treated group, the articular space was destroyed and extensive degeneration of cartilage was observed. Chondrocytes had almost completely disappeared from the femoral condyles as well as from the tibial plateaus. The fatty tissue was replaced by fibrotic tissue, and bone destruction was noted. In the CF101-treated group, the joint space was preserved, and there were minimal degenerative changes. A low number of chondrocytes and few lymphocytes infiltrating the cartilage were noted (Figure 2a, left). Overall, the degree of cartilage damage was markedly lower in the CF101-treated group, as demonstrated by the depth and extent of the damage (Figure 2a, right). The Mankin score was used to further evaluate the cartilage damage. CF101 treatment prevented damage to the cartilage structure, reduced cellular abnormalities, and preserved matrix staining. Overall, CF101 treatment resulted in a 72 ± 14.4% reduction in the Mankin score (mean ± SEM) as compared with the scores in the vehicle-treated animals (Figure 2b).

Safranin O–fast green staining in the vehicle-treated rats revealed extensive destruction of cartilage, with disappearance of chondrocytes. Subchondral bone sclerosis was also noted, with partial replacement of the

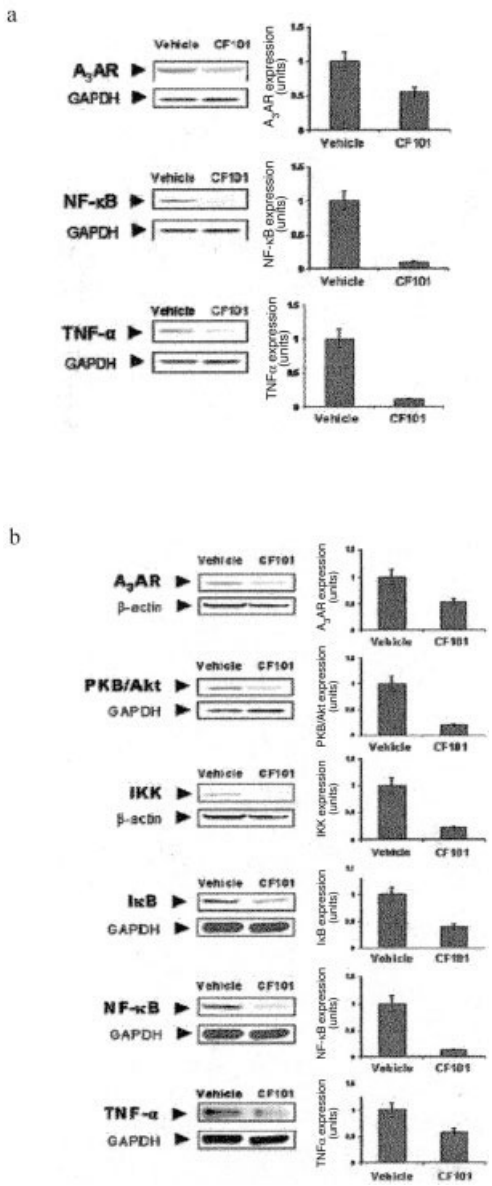

Figure 5. Effect of CF101 on the levels of expression of signaling proteins in knee joint extracts derived from rats with monosodium iodoacetate (MIA)–induced osteoarthritis (OA). Western blot analysis (left) and densitometric analysis of the Western blots (right) were performed on protein extracts from the knee joints of OA rats treated with CF101 or vehicle. **a,** Levels of adenosine A_3 receptor (A_3AR), NF-κB, and tumor necrosis factor α (TNFα) expression on day 15 after MIA injection. Expression of all 3 proteins was decreased in CF101-treated rats as compared with vehicle-treated rats. **b,** Levels of adenosine A_3 receptor, protein kinase B (PKB)/Akt, IKK, IκB, NF-κB, and TNFα at the end of the study. Expression of all 6 proteins was decreased in CF101-treated rats as compared with vehicle-treated rats. Results were normalized against β-actin or GAPDH. Representative Western blots are shown. Densitometric values are the mean and SEM of pooled data from 3 independent experiments (n = 10 joints per group).

bone marrow by fibrotic tissue. In the CF101-treated group, the articular space was preserved, and the cartilage was intact (Figure 2c, left). Moreover, CF101 treatment induced an 80% inhibition in the depth of cartilage damage and a 50% inhibition in the extent of cartilage damage (Figure 2c, right).

Toluidine blue staining revealed that in the vehicle-treated group, the cartilage had almost completely disappeared, and in areas where cartilage was still present, the staining was very pale, demonstrating a loss of proteoglycans. Thickened subchondral bone, with partial replacement of the bone marrow, was also observed. In the CF101-treated group, the histologic structures were preserved, and only a small area showed lighter staining with toluidine blue (Figure 2d, left). Similar to the results obtained with Safranin O–fast green staining, a marked decrease in the depth and extent of cartilage damage was observed following toluidine blue staining in the CF101-treated group (Figure 2d, right).

There was a marked reduction in osteoclast formation and bone destruction in the CF101-treated group (Figure 3a). In addition, CF101 treatment preserved bone trabeculae and bone marrow, whereas vehicle treatment resulted in replacement of bone marrow with proliferating osteoclasts, osteoblasts, and fibrosis (Figure 3b).

In the vehicle-treated group, significant proliferation of synovial cells was observed, and the synovial membrane was expanded with fibroblasts and infiltrated by lymphocytes. In the CF101-treated group, the synovial membrane was preserved, and adipose tissue beneath it was respected (Figure 3c).

The extent of inflammation and pannus formation in the CF101-treated animals was statistically significantly decreased as compared with that in the vehicle-treated animals. Infiltration of mononuclear leukocytes and massive pannus tissue replacing the articular space were noted in the vehicle-treated group, whereas in the CF101-treated group, few lymphocytes were observed, and only traces of pannus tissue were detected (Figure 4).

Effect of CF101 on the expression levels of signaling proteins. Protein extracts were prepared from the knees of CF101-treated and vehicle-treated rats obtained on days 15 and 22 after induction of OA. Western blot analysis revealed down-regulation of A_3 adenosine receptor expression levels at both time points (Figures 5a and b). The decrease in A_3 adenosine receptor expression level shortly after treatment is con-

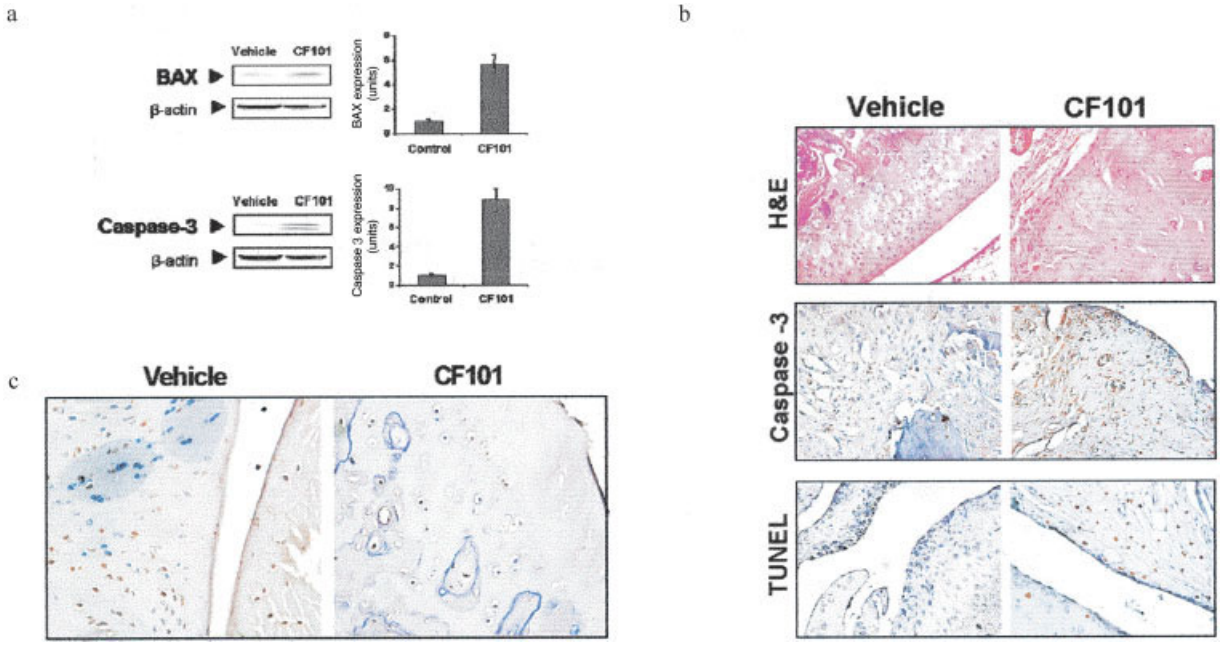

Figure 6. CF101-induced apoptosis of lymphocyte infiltrates, but not chondrocytes, in the knee joints of rats with monosodium iodoacetate–induced osteoarthritis (OA). Knee joints from OA rats treated with CF101 or with vehicle were evaluated with Western blotting, immunohistochemistry, and TUNEL assay. **a,** Bax and caspase 3 expression in protein extracts from the knee joints of OA rats treated with CF101 or vehicle, as determined by Western blotting (left) and densitometric analysis of the Western blots (right). CF101 treatment induced increased expression of both proapoptotic proteins. Representative Western blots are shown. Results were normalized against β-actin. Densitometric values are the mean and SEM of pooled data from 3 independent experiments (n = 10 joints per group). **b,** Immunohistochemical analysis, as determined following hematoxylin and eosin (H&E) staining and anti–caspase 3 treatment, as well as TUNEL assay for cell apoptosis, in the knee joints of OA rats treated with CF101 or vehicle. Caspase 3 expression is weak in the vehicle-treated knee, which is severely infiltrated with inflammatory cells, but in the CF101-treated knee, there is marked expression of caspase 3 in the few infiltrating lymphocytes. TUNEL assay revealed few apoptotic lymphocytes in the severely inflamed vehicle-treated knee, but there are many apoptotic cells in the CF101-treated knee. **c,** TUNEL assay for apoptosis of chondrocytes in the knee joints of OA rats treated with CF101 or vehicle. Apoptotic chondrocytes are present in vehicle-treated rats, whereas no apoptotic chondrocytes are seen in CF101-treated rats. Representative images are shown in **b** and **c** (original magnification $\times$ 40).

sistent with that of other G protein–coupled receptors known to be internalized and degraded upon agonist binding (22).

Next, we examined the expression levels of 2 key signaling proteins that were found to be down-regulated in the CF101-treated group (NF-κB and TNFα) on day 15 after disease induction (Figure 5a). Further analysis at the end of the study (day 22) showed that the expression levels of PKB/Akt, IKK, IκB, NF-κB, and TNFα were decreased in knee protein extracts prepared from the CF101-treated group as compared with those prepared from the vehicle-treated group (Figure 5b).

Western blot analysis demonstrated a significant increase in the expression levels of the proapoptotic proteins Bax and caspase 3 in MIA-injected knees from the rats that had been treated with CF101 (Figure 6a). These results were corroborated by immunohistochemical analysis in which levels of caspase 3 were very low in the knee with severe inflammatory cell infiltration, whereas in the CF101-treated knee, which had low levels of inflammatory cell infiltration, there was robust expression of caspase 3. TUNEL assay performed on a consecutive tissue section demonstrated a few infiltrating lymphocytes undergoing apoptosis in MIA-injected knees from CF101-treated animals, whereas despite a prominent inflammatory reaction in the vehicle-treated rats, little or no apoptosis was present (Figure 6b).

In contrast, apoptotic chondrocytes were observed in the joints of vehicle-treated animals, whereas no apoptosis was detected in chondrocytes in the joints of CF101-treated animals (Figure 6c). These data demonstrate that CF101 treatment protected the rat knees against cartilage loss by preventing the apoptosis of chondrocytes.

DISCUSSION

In the present study, we used a well-established animal model of OA, which was induced by the intra-articular injection of MIA into rat knee joints. MIA disrupts cartilage metabolism, which leads to chondrocyte death and subchondral bone lesions that are consistent with the pathologic changes seen in OA in humans (23). Treatment with CF101, a specific A_3 adenosine receptor agonist, decreased the clinical score for the disease, and administration of MRS1220, a specific A_3 adenosine receptor antagonist, counteracted this effect, demonstrating the specificity of the response. The molecular mechanism of action entailed deregulation of the NF-κB signaling pathway and apoptosis of inflammatory cells.

The oral bioavailability of CF101 has previously been demonstrated in different experimental animal models, both in mice and in rats. CF101 is a highly stable molecule with a proven half-life of 1.4 hours in mice (12–14,16–20). These data prompted the use of twice daily treatment, which resulted in a steady-state blood level of the drug.

CF101 improved the structure of the affected joints, thereby alleviating the development of the disease. More specifically, the impact of CF101 on the development of OA was manifested by a decrease in knee diameter, which was markedly lower in animals treated with oral CF101. In support of the improvement in clinical scores were the radiographic and histopathologic findings showing that CF101 treatment preserved the cartilage, joint space, tibioepiphyseal margin, synovial membrane, and bone marrow and prevented bone destruction and pannus formation. Three different tissue staining methods and analyses were used in these studies, all of which revealed the beneficial effects of CF101 on these different components of the joint.

Analysis of the molecular mechanisms involved in the effects of CF101 revealed that the drug deregulated the NF-κB signaling pathway, which is known to play a major role in the biomechanical and metabolic pathways involved with the etiology and pathogenesis of OA (10,24–26). It has previously been shown that the NF-κB signaling pathway mediates the progression of extracellular matrix damage and cartilage destruction (27). NF-κB was also shown to induce the expression of proinflammatory cytokines, chemokines, and matrix metalloproteinases (MMPs) by human articular chondrocytes (28,29). In addition, mechanical overload has been shown to induce rapid nuclear translocation of NF-κB subunits p65 and p50, resulting in proinflammatory gene induction (30,31).

Deregulation of the NF-κB signaling pathway by CF101 has previously been demonstrated in experimental animal models of RA, including AIA and collagen-induced arthritis (12–14,16,32–34). The current viewpoint expressed in the literature is that some markers of disease activity are similar in OA and RA and that they mainly include some proinflammatory cytokines, such as TNFα, interleukin-1 (IL-1), and MMPs. Up-regulation of NF-κB, the transcription factor for these cytokines, is also a hallmark of both RA and OA (11,35–37). Similarly, with the data showing that CF101 down-regulates NF-κB, TNFα, and IL-1 in cultures of inflammatory cells and in inflammatory tissues from animals with arthritis, CF101 exerted the antiinflammatory effect in OA (12,13,16,18).

Interestingly, a differential effect of CF101 on inflammatory cells and chondrocytes was observed. Apoptosis of inflammatory cells was noted in CF101-treated animals, whereas the drug prevented apoptosis of chondrocytes, which resulted in cartilage protection. It has already been established that apoptosis of chondrocytes may be a result of mechanical injury, loss of extracellular matrix, loss of growth factors, and excessive levels of reactive oxygen species (38,39). The stability and survival of chondrocytes play a crucial role in the preservation of an accurate cartilage matrix. Therefore, the effect of CF101 in preventing chondrocyte apoptosis is an important challenge in the development of potential therapeutic strategies in OA.

NF-κB has been found to be present in the A_3 adenosine receptor gene promoter, and biologic data indicate its role in A_3 adenosine receptor transcription and expression levels (15). Indeed, the data from the current study demonstrate high levels of A_3 adenosine receptor expression in OA knee protein extracts, whereas this expression was down-regulated upon CF101 treatment. We have previously shown that down-regulation of these receptors upon treatment with a selective agonist represents a cellular response to the drug and initiates downstream signal transduction pathways that determine the response to the agonist (12,13). Indeed, our studies have shown that receptor down-regulation is accompanied by a decrease in the expression levels of PKB/Akt, IKK, IκB, NF-κB, and TNFα, leading to an antiinflammatory effect and improvement in disease manifestations (12–16). It may be suggested that NF-κB acting via an autocrine pathway regulates both receptor expression and functionality and acts as an important mediator of the cellular response to CF101.

Pain in OA joints has been attributed to different causes that are secondary to the anatomical changes, such as inflammatory events in the synovium as well as subchondral intraosseous hypertension due to venous congestion (11,30–42). Interestingly, IB-MECA (CF101) was shown to exert an inhibitory effect on the release of pain-related neuropeptides in the spinal cord via its binding to the spinal A_3 adenosine receptor, which resulted in a reduction of the late-phase response of formalin-induced inflammatory hyperalgesia (43).

We have demonstrated in the present study that treatment of OA with CF101, an A_3 adenosine receptor agonist, is efficacious. The molecular mechanism involves deregulation of the NF-κB signaling pathway and apoptosis of inflammatory cells. Based on the data presented herein, CF101 appears to alter the course of the disease and may be suggested to be a disease-modifying OA drug.

AUTHOR CONTRIBUTIONS

All authors were involved in drafting the article or revising it critically for important intellectual content, and all authors approved the final version to be published. Dr. Fishman had full access to all of the data in the study and takes responsibility for the integrity of the data and the accuracy of the data analysis.

Study conception and design. Bar-Yehuda, Ochaion, Cohen, Fishman.
Acquisition of data. Rath-Wolfson, Del Valle, Patoka, Zozulya, Barer, Atar, Piña-Oviedo, Perez-Liz, Castel.
Analysis and interpretation of data. Bar-Yehuda, Ochaion, Cohen, Fishman.

REFERENCES

1. Martel-Pelletier J, Boileau C, Pelletier JP, Roughley PJ. Cartilage in normal and osteoarthritis conditions. Best Pract Res Clin Rheumatol 2008;22:351–84.
2. Sowers M. Epidemiology of risk factors for osteoarthritis: systemic factors. Curr Opin Rheumatol 2001;13:447–51.
3. Hardingham T. Extracellular matrix and pathogenic mechanisms in osteoarthritis. Curr Rheumatol Rep 2008;10:30–6.
4. Baddour VT, Bradley JD. Clinical assessment and significance of inflammation in knee osteoarthritis. Curr Rheumatol Rep 1999;1: 59–63.
5. Fernandes JC, Martel-Pelletier J, Pelletier JP. The role of cytokines in osteoarthritis pathophysiology. Biorheology 2002;39: 237–46.
6. McMahon K, Nelson M, Jones G. Treating the symptoms of osteoarthritis—oral treatments. Aust Fam Physician 2008;37: 133–5.
7. Chen YF, Jobanputra P, Barton P, Bryan S, Fry-Smith A, Harris G, et al. Cyclooxygenase-2 selective non-steroidal anti-inflammatory drugs (etodolac, meloxicam, celecoxib, rofecoxib, etoricoxib, valdecoxib and lumiracoxib) for osteoarthritis and rheumatoid arthritis: a systematic review and economic evaluation. Health Technol Assess 2008;12:1–278, iii.
8. Malemud CJ, Schulte ME. Is there a final common pathway for arthritis? Future Rheumatol 2008;3:253–68.
9. Pelletier JP, Martel-Pelletier J, Abramson SB. Osteoarthritis, an inflammatory disease: potential implication for the selection of new therapeutic targets [review]. Arthritis Rheum 2001;44: 1237–47.
10. Roman-Blas JA, Jimenez SA. NF-κB as a potential therapeutic target in osteoarthritis and rheumatoid arthritis. Osteoarthritis Cartilage 2006;14:839–48.
11. Furuzawa-Carballeda J, Macip-Rodriguez PM, Cabral AR. Osteoarthritis and rheumatoid arthritis pannus have similar qualitative metabolic characteristics and pro-inflammatory cytokine response. Clin Exp Rheumatol 2008;26:554–60.
12. Fishman P, Bar-Yehuda S, Madi L, Rath-Wolfson L, Ochaion A, Cohen S, et al. The PI3K–NF-κB signal transduction pathway is involved in mediating the anti-inflammatory effect of IB-MECA in adjuvant-induced arthritis. Arthritis Res Ther 2006;8:R33.
13. Rath-Wolfson L, Bar Yehuda S, Madi L, Ochaion A, Cohen S, Zabutti A, et al. IB-MECA, an A_3 adenosine receptor agonist prevents bone resorption in rats with adjuvant induced arthritis. Clin Exp Rheumatol 2006;24:400–6.
14. Ochaion A, Bar-Yehuda S, Cohn S, Del Valle L, Perez-Liz G, Madi L, et al. Methotrexate enhances the anti-inflammatory effect of CF101 via up-regulation of the A_3 adenosine receptor expression. Arthritis Res Ther 2006;8:R169.
15. Madi L, Cohn S, Ochaion A, Bar-Yehuda S, Barer F, Fishman P. Over-expression of A_3 adenosine receptor in peripheral blood mononuclear cells of rheumatoid arthritis: involvement of NF-κB in mediating receptor level. J Rheumatol 2007;34:20–6.
16. Bar-Yehuda S, Silverman MH, Kerns WD, Ochaion A, Cohen S, Fishman P. The anti-inflammatory effect of A_3 adenosine receptor agonists: a novel targeted therapy for rheumatoid arthritis. Expert Opin Investig Drugs 2007;16:1601–13.
17. Ochaion A, Bar-Yehuda S, Cohen S, Amital H, Jacobson KA, Joshi BV, et al. The A_3 adenosine receptor agonist CF502 inhibits the PI3K, PKB/Akt and NF-κB signaling pathway in synoviocytes from rheumatoid arthritis patients and in adjuvant-induced arthritis rats. Biochem Pharmacol 2008;76:482–94.
18. Baharav E, Bar-Yehuda S, Madi L, Silberman D, Rath-Wolfson L, Halpern M, et al. The anti-inflammatory effect of A_3 adenosine receptor agonists in murine autoimmune arthritis models. J Rheumatol 2005;32:469–76.
19. Van Troostenburg AR, Clark EV, Carey WD, Warrington SJ, Kerns WD, Cohn I, et al. Tolerability, pharmacokinetics, and concentration-dependent hemodynamic effects of oral CF101, an A_3 adenosine receptor agonist, in healthy young men. Int J Clin Pharmacol Ther 2004;42:534–42.
20. Silverman MH, Strand V, Markovits D, Nahir M, Reitblat T, Molad Y, et al. Clinical evidence for utilization of the A_3 adenosine receptor as a target to treat rheumatoid arthritis: data from a phase II clinical trial. J Rheumatol 2008;35:41–8.
21. Mankin HJ, Dorfman H, Lippiello L, Zarins A. Biochemical and metabolic abnormalities in articular cartilage from osteo-arthritic human hips. II. Correlation of morphology with biochemical and metabolic data. J Bone Joint Surg Am 1971;53:523–37.
22. Schmid SL, Fuchs R, Male P, Mellman I. Two distinct subpopulations of endosomes involved in membrane recycling and transport to lysosomes. Cell 1988;52:73–83.
23. Guingamp C, Gegout-Pottie P, Philippe L, Terlain B, Netter P, Gillet P. Mono-iodoacetate–induced experimental osteoarthritis: a dose–response study of loss of mobility, morphology, and biochemistry. Arthritis Rheum 1997;40:1670–9.
24. Berenbaum F. Signaling transduction: target in osteoarthritis. Curr Opin Rheumatol 2004;16:616–22.
25. Saklatvala J. Inflammatory signaling in cartilage: MAPK and NF-κB pathways in chondrocytes and the use of inhibitors for research into pathogenesis and therapy of osteoarthritis. Curr Drug Targets 2007;8:305–13.
26. Liacini A, Sylvester J, Li WQ, Zafarullah M. Inhibition of interleukin-1-stimulated MAP kinases, activating protein-1 (AP-1) and nuclear factor κB (NF-κB) transcription factors down-regulates

matrix metalloproteinase gene expression in articular chondrocytes. Matrix Biol 2002;21:251–62.
27. Liacini A, Sylvester J, Li WQ, Huang W, Dehnade F, Ahmad M, et al. Induction of matrix metalloproteinase-13 gene expression by TNF-α is mediated by MAP kinases, AP-1, and NF-κB transcription factors in articular chondrocytes. Exp Cell Res 2003;288: 208–17.
28. Pulai JI, Chen H, Im HJ, Kumar S, Hanning C, Hegde PS, et al. NF-κB mediates the stimulation of cytokine and chemokine expression by human articular chondrocytes in response to fibronectin fragments J Immunol 2005;174:5781–8.
29. Forsyth CB, Cole A, Murphy G, Bienias JL, Im HJ, Loeser RF Jr. Increased matrix metalloproteinase-13 production with aging by human articular chondrocytes in response to catabolic stimuli. J Gerontol A Biol Sci Med Sci 2005;60:1118–24.
30. Deschner J, Hofman CR, Piesco NP, Agarwal S. Signal transduction by mechanical strain in chondrocytes. Curr Opin Clin Nutr Metab Care 2003;3:289–93.
31. Agarwal S, Long P, Seyedain A, Piesco N, Shree A, Gassner R. A central role for the nuclear factor-κB pathway in anti-inflammatory and proinflammatory actions of mechanical strain. FASEB J 2003;17:899–901.
32. Seguin CA, Bernier SM. TNFα suppresses link protein and type II collagen expression in chondrocytes: role of MEK1/2 and NF-κB signaling pathways. J Cell Physiol 2003;197:356–69.
33. Tomita T, Takeuchi E, Tomita N, Morishita R, Kaneko M, Yamamoto K, et al. Suppressed severity of collagen-induced arthritis by in vivo transfection of nuclear factor κB decoy oligodeoxynucleotides as a gene therapy. Arthritis Rheum 1999;42: 2532–42.
34. Yin H, Zhang F, Yu M, Cheng H, Lin J, Gao Y, et al. β-endorphin ameliorates synovial cell hyperfunction in the collagen-induced arthritis rat model by specific downregulation of NF-κB activity. Neuroendocrinology 2005;81:10–8.
35. Arii K, Kumon Y, Sugahara K, Nakatani K, Ikeda Y, Suehiro T, et al. Edaravone inhibits collagen-induced arthritis possibly through suppression of nuclear factor-κB. Mol Immunol 2008;45: 463–9.
36. Shaw T, Nixon JS, Bottomley KM. Metalloproteinase inhibitors: new opportunities for the treatment of rheumatoid arthritis and osteoarthritis. Expert Opin Investig Drugs 2000;9:1469–78.
37. Van den Berg WB. The role of cytokines and growth factors in cartilage destruction in osteoarthritis and rheumatoid arthritis. Z Rheumatol 1999;58:136–41.
38. Mistry D, Oue Y, Chambers MG, Kayser MV, Mason RM. Chondrocyte death during murine osteoarthritis. Osteoarthritis Cartilage 2004;12:131–41.
39. Del Carlo M Jr, Loeser RF. Cell death in osteoarthritis. Curr Rheumatol Rep 2008;10:37–42.
40. Jacques C, Gosset M, Berenbaum F, Gabay C. The role of IL-1 and IL-1Ra in joint inflammation and cartilage degradation. Vitam Horm 2006;74:371–403.
41. Felson D. The sources of pain in knee osteoarthritis. Curr Opin Rheumatol 2005;17:624–8.
42. Hinz B, Brune K. Pain and osteoarthritis: new drugs and mechanisms. Curr Opin Rheumatol 2004;16:628–33.
43. Yoon MH, Bae HB, Choi JI. Antinociception of intrathecal adenosine receptor subtype agonists in rat formalin test. Anesth Analg 2005;101:1417–21.

DOI 10.1002/art.25049

Erratum

In the article by Damjanov et al in the May 2009 issue of *Arthritis & Rheumatism* (pages 1232–1241), the graph in the upper right panel of Figure 2 was incorrect. This error did not affect the interpretation or conclusions of the study. A corrected figure is shown below.

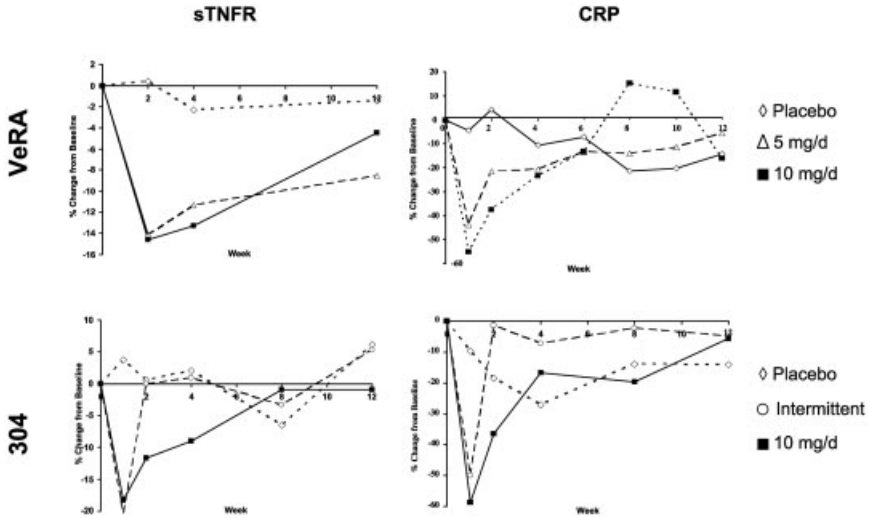

Figure 2. Median percent change from baseline (BL) in the levels of the soluble 55-kd isoform of tumor necrosis factor receptor (sTNFRp55) and C-reactive protein (CRP) over time in the VeRA study and Study 304.

We regret the error.